ACCOUNTS
of chemical research

Aggregate Nanostructures of Organic Molecular Materials

HUIBIAO LIU, JIALIANG XU, YONGJUN LI, AND YULIANG LI*

CAS Key Laboratory of Organic Solid, Beijing National Laboratory for Molecular Sciences (BNLMS), Institute of Chemistry, Chinese Academy of Sciences, Beijing 100190, P. R. China

RECEIVED ON JUNE 12, 2010

CONSPECTUS

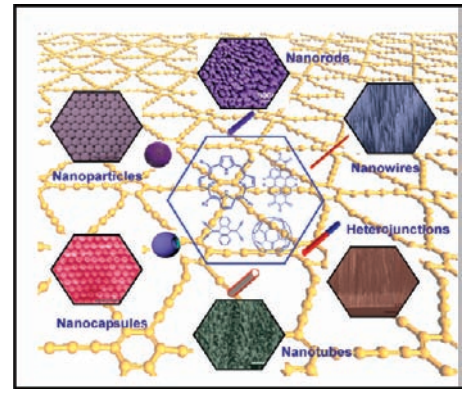

Conjugated organic molecules are interesting materials because of their structures and their electronic, electrical, magnetic, optical, biological, and chemical properties. However, researchers continue to face great challenges in the construction of well-defined organic compounds that aggregate into larger molecular materials such as nanowires, tubes, rods, particles, walls, films, and other structural arrays. Such nanoscale materials could serve as direct device components. In this Account, we describe our recent progress in the construction of nanostructures formed through the aggregation of organic conjugated molecules and in the investigation of the optical, electrical, and electronic properties that depend on the size or morphology of these nanostructures.

We have designed and synthesized functional conjugated organic molecules with structural features that favor assembly into aggregate nanostructures via weak intermolecular interactions. These large-area ordered molecular aggregate nanostructures are based on a variety of simpler structures such as fullerenes, perylenes, anthracenes, porphyrins, polydiacetylenes, and their derivatives. We have developed new methods to construct these larger structures including organic vapor−solid phase reaction, natural growth, association via self-polymerization and self-organization, and a combination of self-assembly and electrochemical growth. These methods are both facile and reliable, allowing us to produce ordered and aligned aggregate nanostructures, such as large-area arrays of nanowires, nanorods, and nanotubes. In addition, we can synthesize nanoscale materials with controlled properties. Large-area ordered aggregate nanostructures exhibit interesting electrical, optical, and optoelectronic properties.

We also describe the preparation of large-area aggregate nanostructures of charge transfer (CT) complexes using an organic solid-phase reaction technique. By this process, we can finely control the morphologies and sizes of the organic nanostructures on wires, tubes, and rods. Through field emission studies, we demonstrate that the films made from arrays of CT complexes are a new kind of cathode materials, and we systematically investigate the effects of size and morphology on electrical properties.

Low-dimension organic/inorganic hybrid nanostructures can be used to produce new classes of organic/inorganic solid materials with properties that are not observed in either the individual nanosize components or the larger bulk materials. We developed the combined self-assembly and templating technique to construct various nanostructured arrays of organic and inorganic semiconductors. The combination of hybrid aggregate nanostructures displays distinct optical and electrical properties compared with their individual components. Such hybrid structures show promise for applications in electronics, optics, photovoltaic cells, and biology.

In this Account, we aim to provide an intuition for understanding the structure−function relationships in organic molecular materials. Such principles could lead to new design concepts for the development of new nonhazardous, high-performance molecular materials on aggregate nanostructures.

Published on the Web 10/13/2010 www.pubs.acs.org/acr
10.1021/ar100084y

1. Introduction

Organic conjugated molecular materials, also referred to as organic semiconductors, with a delocalized π-electron system have an "intrinsic" wide band gap that defines their affinity for electrons.[1] During the past decade, aggregate nanostructures of organic molecules have attracted significant attention due to their promising applications in light-emitting diodes, photovoltaic cells, sensors, lasers, field emitters, and field-effect transistors.[2−9] There is currently an intensive effort to develop methods for producing organic aggregation materials with low-dimensionality structures such as nanowires, nanotubes, and nanorods, which are of great importance in the development of optoelectronic and nanoelectronic devices. Recently, scientists have developed techniques for synthesizing and characterizing many new organic semiconductors of nanowires and nanotubes and other nanostructures with at least one dimension on the nanoscale by various methods.[3−12] These novel aggregation structures and materials have been driven by their unique properties, as well as by the processing advantages of organic electronic materials relative to inorganic electronic materials. Typically during this phase of development of a new technology area, researchers focus mainly on identifying new properties and understanding the structure−properties relationships that relate specifically to aggregate nanostructures and materials leading to new architectures for producing benign, high-performance nanoscale substances. These materials are expected to (i) exhibit the relationships of structure−function, (ii) exhibit new size-based properties, and (iii) provide compelling reasons for functionality and applications. However, still, the design and synthesis of novel aggregate nanostructures of conjugated organic molecules with well-defined morphology and size and controlled properties is a significant and ongoing challenge within nanoscience and nanotechnology.

This Account is organized as follows. First, we briefly summarize the construction and properties of well-defined aggregation structures of organic conjugated molecules on nanometer scale. We explore the application of aggregation chemistry principles to the field of nanoscience and the applicability of the strategies of aggregation chemistry to control the size, shape, and dimension of organic semiconductor molecules. Then, we further focus the Account on those methods that assemble nanostructure building blocks and the dimension (morphologies or size)-dependent optical and electronic properties of those aggregated nanostructures. Combination of semiconductor organic molecules and semiconductor inorganic molecules produced new nanostructure hybrid materials. For the purpose of this Account, we will primarily focus on the fabrication of organic/inorganic p−n junction nanowires and investigation of photo-induced energy/charge transport at the organic/inorganic interface that might also serve as electric power in the nanoscale circuit.

The Account not only demonstrates the increasing emerging research of aggregated nanostructures of organic conjugated molecules but also provides new insights into how to combine the factors of molecular structures, energy levels, and properties to achieve the construction of well-defined aggregation structures of organic conjugated molecules for the preparation of highly functionalized materials.

2. Self-Assembled Aggregate Nanostructures of Organic Conjugated Systems

2.1. Self-Assembled Aggregate Nanostructures of Conjugated Small Molecules. There is currently an intensive effort to develop methods for producing materials with two-dimensionally (2D) or three-dimensionally (3D) structured patterns and arrays, which are of great importance and interest because of their potential applications in the development of optoelectronic and microelectronic devices and the fabrication of chemical and biological sensors.[13] In the most recent developments, the fabrication of 2D or 3D structured patterns and arrays of porphyrins via colloidal self-assembly is particularly attractive.[2,13]

Porphyrins are attractive building blocks for organic nanostructures because of their unique electronic, optical, catalytic, and biochemical properties. The self-assembly of porphyrin derivatives has therefore become a widely investigated topic.[2,13−17] However, how to tune the aggregate structures of the porphyrin molecules and control the self-assembly process for producing the different dimensions of nanostructures are of great importance and interest. In our investigation, high-quality ordered 2D and 3D patterns and well-defined arrays including fibers, vesicles, and tubular structures have been fabricated from porphyrin derivative building blocks with the assistance of nonconvalent weak interactions such as hydrogen-bonding, $\pi-\pi$ stacking, and electrostatic interactions and metal−ligand bonds.[14−17] A novel linear amphiphilic porphyrin derivative (bpy−ZnP−pyridine) composed of two porphyrins connected with 2,2′-bipyridyl group was synthesized and showed a V-shaped conformer after the 2,2′-bipyridine group was complexed with palladium(II) dichloride. The complex showed perfect structure of spherical vesicles with a uniform diameter of about 200 nm.[14] The membrane-wall thickness of

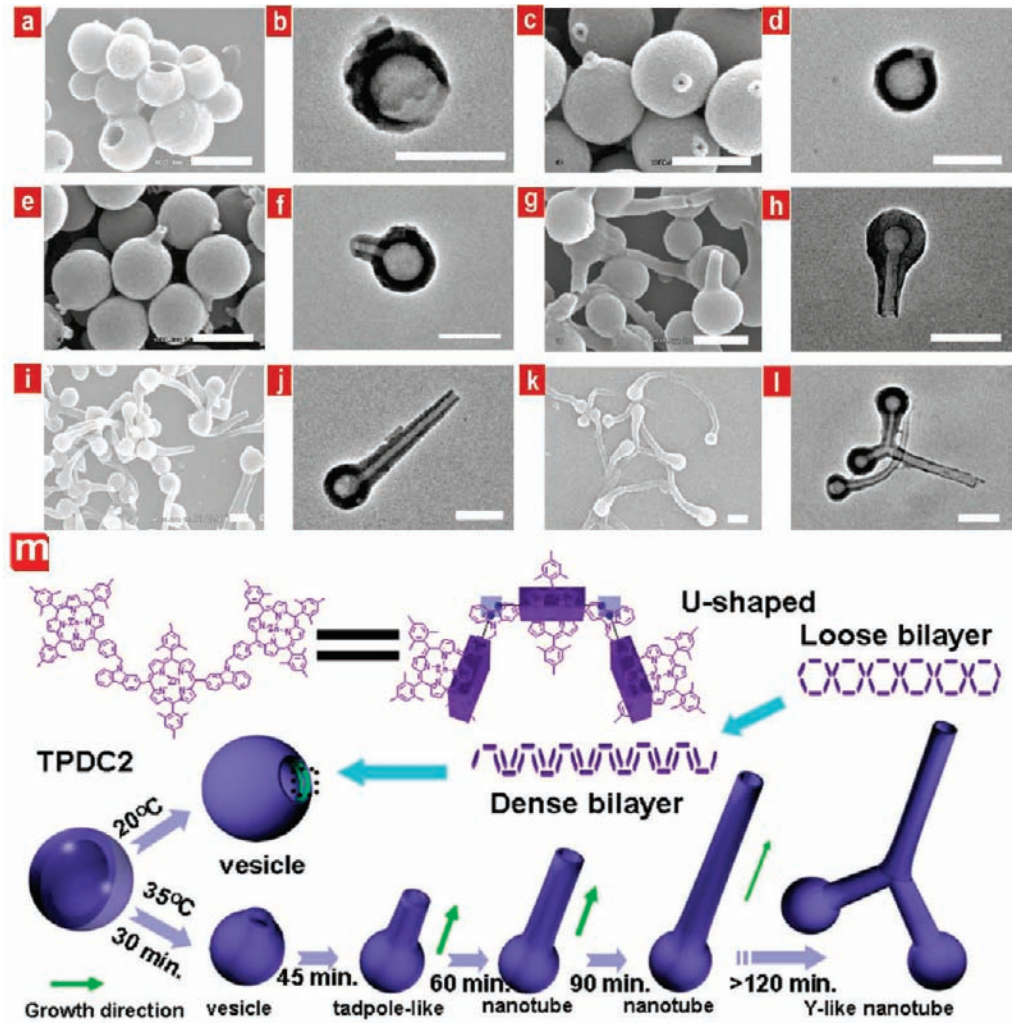

FIGURE 1. SEM and TEM images of the U-type molecule **TPDC2** at (a,b) 20 °C for 30 min or at 35 °C for (c,d) 30, (e,f) 45, (g,h) 60, (i,j) 90, and (k,l) more than 120 min. Scale bars = 500 nm. (m) Schematic of natural growth process of the TPCD2 vesicles.

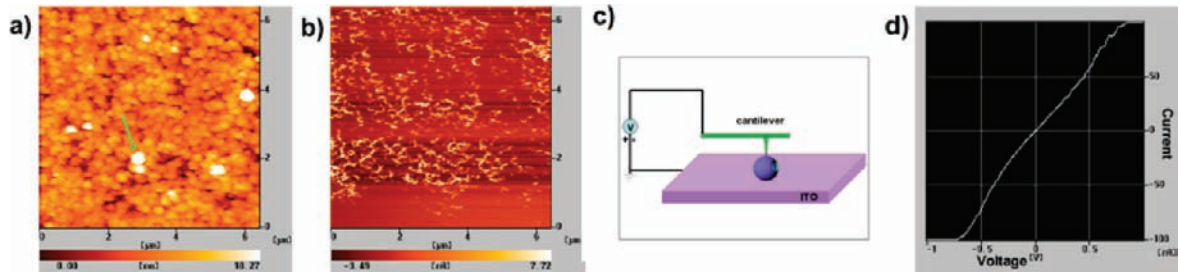

FIGURE 2. Conductive property: (a) the morphology, (b) current AFM image of the **TPDC2** vesicle sample, (c) schematic experimental setup, and (d) the *I*−*V* curves of the **TPDC2** vesicle.

the vesicles was measured to be 15−20 nm, fitting approximately with two to three bilayers of bpy−ZnP−pyridine with a molecular dimension of 12−18 nm. Both the Soret and Q absorption bands of the vesicle structured films were broadened and red-shifted, suggesting "J-type" (edge-to-edge) supramolecular interaction of the porphyrin derivative in the vesicles. This amphiphilic molecule assembled into layered structures and then closed to form vesicles. A U-shaped porphyrin derivative, **TPDC2**, was grown into 0D tadpole-like vesicles and finally into 1D nanotubes or multidimensional Y-like nanotubes (Figure 1A,B).[15] The $\pi-\pi$ stacking between the porphyrin triads was suggested to be the major driving force in the self-assembly procedure. In the mixture of CH_2Cl_2/CH_3OH, methanol coordinated with the zinc porphyrin units and **TPDC2** self-assembled into J-type aggregates, leading to a bilayer structure. The increased temperature accelerated the

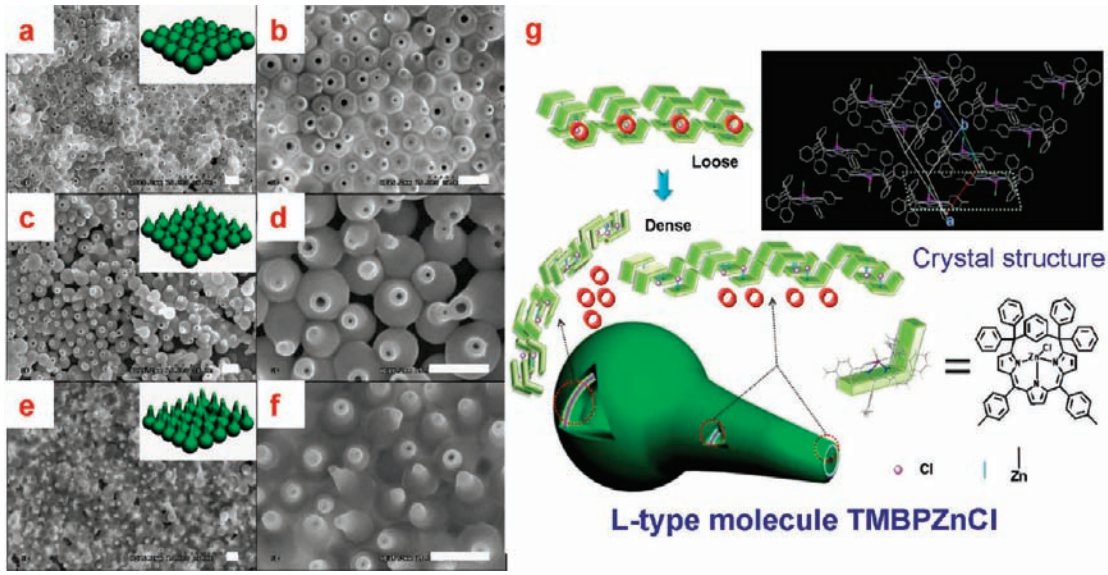

FIGURE 3. SEM images of **TMBPZnCl** prepared in CH_2Cl_2/CH_3OH (1:1) for (a,b) 4 min, (c,d) 8 min, and (e,f) 12 min. The scale bar is 1 mm. (g) Schematic representation of the L-type molecule **TMBPZnCl** block shows the stack of the hollow structured membranes.

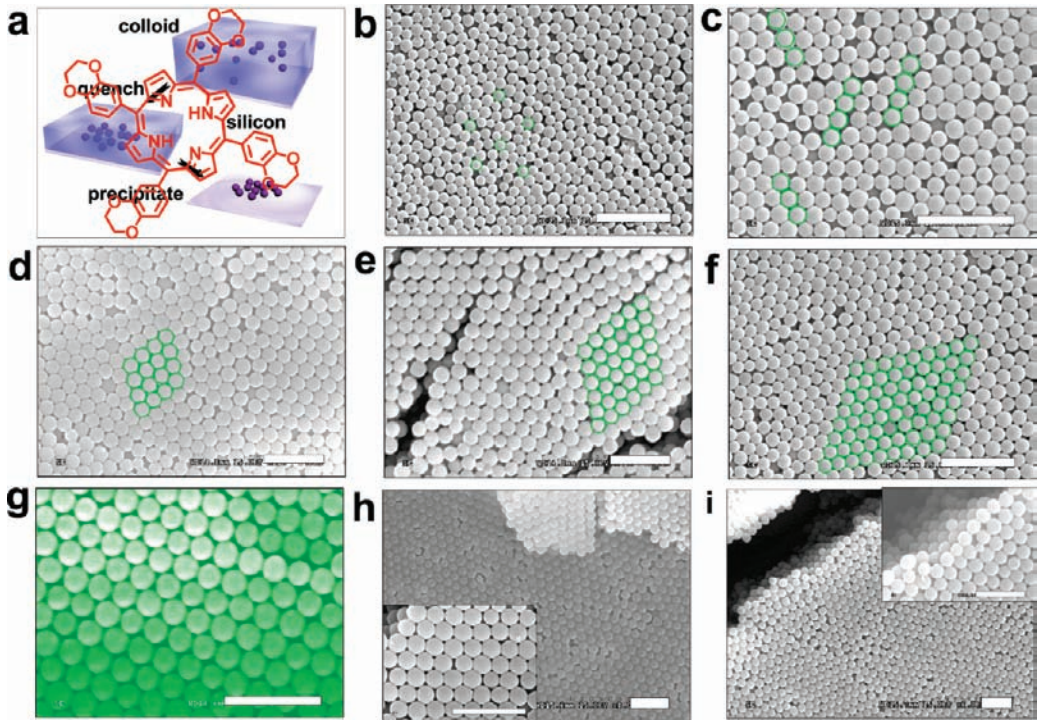

FIGURE 4. (a) Schematic outline and SEM images of **TEOP** pattern prepared by thermal treatment mode I for (b) 5 min, (c) 6 min, (d) 7 min, (e) 8 min, (f) 9 min, and (g) 10 min and (h) layer by layer assembly and (c) multilayer assembly of **TEOP** film. Scale bars = 2 μm.

escape rate of methanol from spherical vesicles, resulting in the formation of protuberant morphology along the edges of the hole. The conductive properties of the individual **TPDC2** vesicles have been investigated by atomic force microscopy (AFM) using a conductive cantilever indicating their organic semiconducting properties (Figure 2).

The L-shaped porphyrin analogue of **TMBPZnCl** was employed as a building block that is able to produce hollow nanostructures with diverse morphologies of low-dimensional to multidimensional (Figure 3) structures by an evaporation-driven self-assembly process.[16] In this process, the growth time and temperature played key roles in determining the self-assembly of the typical hollow nanostructures. Series of vesicle structures with diverse morphologies ranging from low-dimensional vesicles to multidimensional Ω-like vesicles were obtained and finally formed into arrayed patterns. Two or

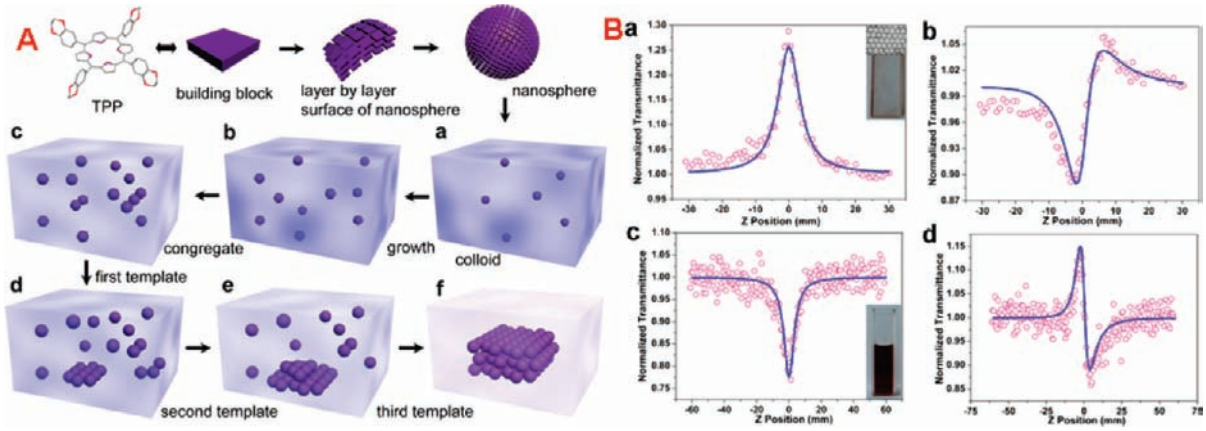

FIGURE 5. (A) Schematic outline of the growth and assembly procedure of **TEOP** film with ordered pattern and (B) NLO properties of (a,b) the **TEOP** well-ordered films and (c,d) the **TEOP** solution.

SCHEME 1. Schematic Illustration of the Template Synthesis of Fullerene Nanotubes

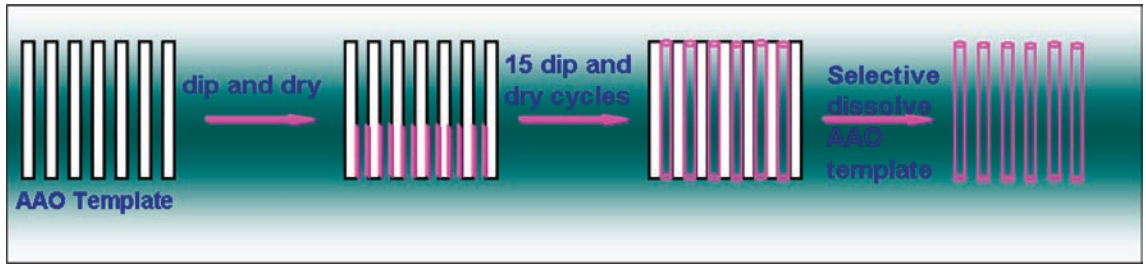

three-dimensional structured nanopatterns and arrays can be fabricated via the colloidal self-assembly process of a novel porphyrin molecule of TEOP (Figure 4a).[17] The procedure described here is remarkable for its simplicity and effectiveness in forming ordered array films with large areas. Both nonlinear absorption and nonlinear refraction of the TEOP film with ordered pattern and TEOP solution were studied using the Z-scan technique. The novel TEOP film architecture exhibits great potential applications for new optical devices. The diameter of ordered uniform nanospheres is about 560 nm, close-packed in a hexagonal lattice. Detailed observation of the self-assembly processes demonstrated that all of the ordered pattern was formed via a progressive process with the diameter of the nanospheres increasing gradually (Figure 4b−g). The large areas of the ordered patterns were formed based on the alignment of the ordered nanospheres in a self-assembly time of 10 min. The 3D ordered patterns were assembled layer by layer, and the thickness of those patterns is about 1.2 μm (Figure 4h). While the concentration of the TEOP solution injected onto the surface of the silicon slice increased to 10^{-2} M, multilayer thicknesses of the 3D ordered pattern were constructed (Figure 4i). The layers of the nanospheres were controlled by growth time and concentration, and the TEOP nanospheres formed a face-centered cubic pattern (Figure 5A). Nonlinear optical (NLO) measurements of these well-ordered TEOP films (Figure 5B) showed that the film possessed saturation absorption with a nonlinear absorption coefficient β of -4.3×10^{-6} m/W and the nonlinear refraction coefficient n_2 of 2.8×10^{-13} m^2/W, respectively. In contrast, the nonlinear absorption of TEOP solution in DMF was a self-defocusing reverse saturation absorption with $\beta = 1.5 \times 10^{-9}$ m/W and $n_2 = -2.53 \times 10^{-16}$ m^2/W, which was 3 orders of magnitude weaker than that of the ordered films.[17]

We have first developed a useful and experimentally easy way to directly fabricate C_{60} nanotubes with a monodisperse size distribution and uniform orientation using C_{60} powders (Scheme 1).[18] Aligned C_{60} nanotubes were observed with smooth and clean surfaces, diameters of 220−310 nm and lengths of 60 μm. TEM examinations demonstrated that the nanotubes were polycrystalline in nature, and the structure of nanotubes was a mixed phase of face-centered cubic and hexagonal close-packed structure. A fullerene derivative of $C_{60}(O)(OO^tBu)_4$ was facilely fabricated into nanotubes with much fewer "dip-and-dry" cycles because of the excellent solubility of the fullerene derivative in chloroform. Fullerene nanotubes therefore are formed at higher temperature by pyrogenic decomposition of the fullerene derivative nanotubes.[19]

In our recent works, we developed a novel technique for a solid-phase organic reaction integrated VS process for grow-

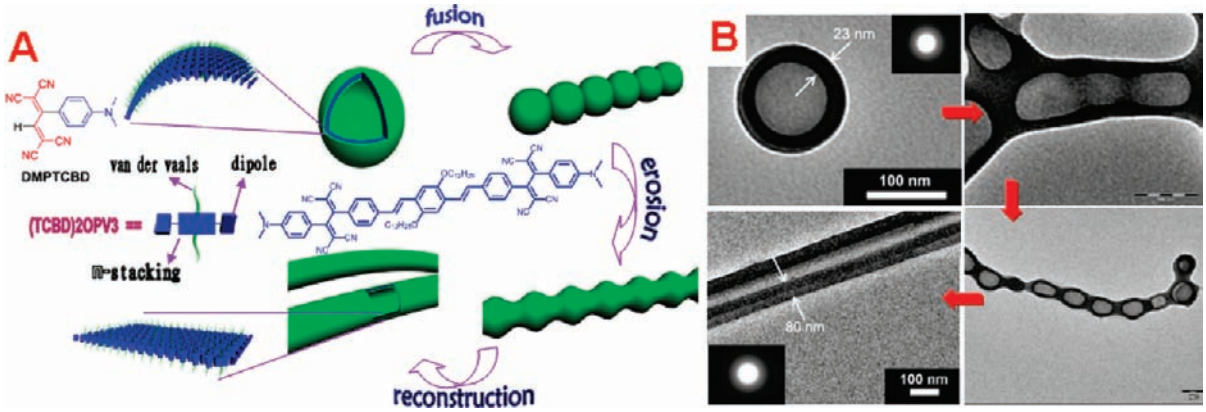

FIGURE 6. (A) Schematics of the $(TCBD)_2OPV_3$ nanostructure formation and morphology transition process and (B) intermediates of the morphology transition.

ing organic 1D nanomaterials.[20,21] In the integrated method, the supersaturation ratio was controlled by the rate of solid-phase organic reaction. The method has been proven to be a general method for fabrication of organic 1D nanomaterials with high crystallinity. 9-Anthracenecarboxylic acid and CaO were reacted to afford anthracene (AN) nanowires with clean and smooth surfaces by the associated approach with lengths of tens of micrometers and diameters in the range of tens of nanometers to several micrometers. The rod-like perylene (PY) nanostructures were also synthesized by similar solid-phase reaction of 3,4,9,10-perylenetetracarboxylic dianhydride and BaO. X-ray diffraction patterns (XRD) showed that the AN nanowires were monoclinic crystalline with preferential orientation along the *a*-axis and the PY nanorods were α-perylene crystal. The AN and PY molecules display the dimension-dependent emission properties observed in the AN nanowires and PY nanorods. The emission of AN nanowires showed sharp luminescence centered at 443 nm due to the growth orientation along the *a*-axis, and there is scarcely any excimer in the AN nanowires. The PY nanorods showed only one excimer emission at 625 nm because the major building units of PY nanorods are the ideal dimeric α-phase packing configuration.[20]

Intramolecular charge-transfer (ICT) compounds often have an electron donor (D) and an electron acceptor (A) connected by a π-conjugated bridge. Such D−A-substituted conjugated molecules are highly polarized and widely used as NLO materials, red emitters, and organic light-emitting diodes.[22−25] However, most of these D−A-substituted red emitters suffer an aggregation-caused emission quenching (ACQ) in the solid phase, which greatly limits their applications. We designed an OPV_3-bridged ICT compound of $(TCBD)_2OPV_3$. The compound is able to undergo a morphology transition in the self-assembling process from 0D hollow nanospheres to 1D nanotubes (Figure 6).[22] The self-assembly behaviors of the model ICT compound DMPTCBD with the same donor−acceptor pairs as $(TCBD)_2OPV_3$ were examined. The result showed a similar morphology transition from 0D to 1D nanostructures. Therefore, the morphology transition and reconstruction processes are proposed to be a "curvature strain releasing" process driven by donor−acceptor dipole−dipole interactions. Both aggregates of vesicles and nanotubes were observed to be aggregation-induced emission enhancement (AIEE)-active with good red emission and near-infrared end emission of 750−850 nm. Further investigation of the effect of the dipole−dipole interactions on the self-assembly behaviors showed that ICT compounds self-assembly into rather distinct aggregated superstructures was driven by asymmetrical and symmetrical dipole−dipole interactions.[23] By employing the self-assemblies of the ICT compound **DMPFM**, a stepwise growth method has been developed for constructing micro/nanohierarchical crystal superarchitectures (Figure 7).[24]

2.2. Self-Assembled Aggregate Nanostructures of Organic π-Conjugated Polymers. Polydiacetylenes are one of the most widely investigated conjugated polymers because of their quasi-1-D electronic structure, fast and largely nonlinear responses, and very fast photoconducting properties.[11,26] The self-assembly of organic molecules with the assistance of noncovalent forces provides an efficient method for creating organic 1D nanostructures. Recently, we have developed a facile method based on the associated effect of self-polymerization and self-assembly for construction of nanoscale supramolecular materials of polymers[26] The monomer 6-carbazol-9-ylhexa-2,4-diyl-1-ol (CYDIOL) was first self-assembled into 1D nanostructures with the help of $\pi-\pi$ stacking and H-bonding interactions. The polymer can form large-scale ordered nanowires on the surface of copper foil. When the foil was irradiated with UV light for 2 h, nanowires with diame-

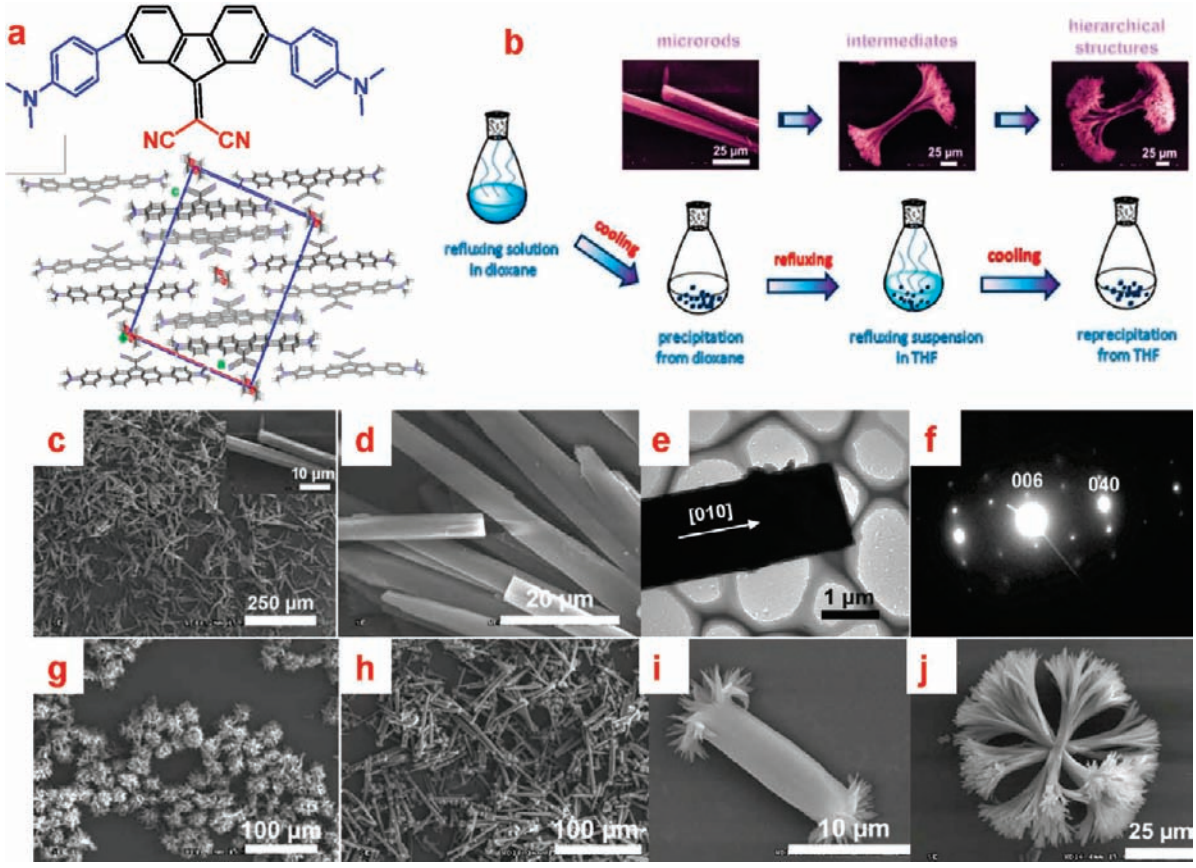

FIGURE 7. (a) DMPFM molecule and crystal structure, (b) schematics of the stepwise growth procedure, (c−f) SEM and TEM images of microrods, and SEM images of (g) microflowers and (h−j) hierarchical microstructures.

ter of 50−120 nm and length of several micrometers were obtained. The field emission (FE) property showed that the turn-on field (E_{to}) of the poly-CYDIOL nanowires film was 8.2 V/μm at 10 μA/cm^2 and the maximum current density is larger than 5 mA/cm^2. The work function of the poly-CYDIOL nanowires is around 3.05 eV, which is much smaller than that of graphite (4.34 eV).

Carbon−carbon triple-bonded (sp-hybridized) graphdiyne was proposed to be a novel structure in the carbon family and predicted to be the most stable of the various diacetylenic nonnatural carbon allotropes. In our recent work, we have synthesized a new carbon allotrope-graphdiyne in a large-scale via a cross-coupling reaction from hexaethynylbenzene (Figure 8).[27] The graphdiyne film was successfully grown on the surface of copper foil in the presence of pyridine by a cross-coupling reaction. Cu served both as a catalyst and a substrate for growing graphdiyne film. The flexible films were about 1 μm in thickness and were composed of graphdiyne multilayers. HRTEM observations exhibited clear lattice fringes of 4.19 Å of graphdiyne films without defects or dislocations, which is larger than that of grapheme (2.32 Å) and graphite (2.46 Å). The selective area electron diffraction pattern (SAED) and XRD patterns definitely confirmed the nature of high crystallinity. The devices based on graphdiyne films on the Cu foil were fabricated for conductivity studies and the $I-V$ curve of the graphdiyne film, which exhibited Ohmic behavior, was linear and the slope of the line is 2.53×10^{-3} with the conductivity calculated as 2.516×10^{-4} S m^{-1}, comparable to silicon, demonstrating the excellent semiconducting properties.

3. Self-Assembled Aggregate Nanostructures of Organic Charge Transfer (CT) Complexes

Organic charge transfer complexes of AgTCNQ and CuTCNQ (TCNQ = 7,7,8,8-tetracyanoquinodimethane) have been identified to have potential applications in diverse fields such as molecular electronic devices, optical switching, electrical recording media, and nonlinear optical devices.[28−31] We have successfully prepared large-area (28.8 cm^2, 48.6 cm^2) AgTCNQ and CuTCNQ nanowires on the surface of Ag and Cu foils by organic vapor−solid-phase reactions (Figure 9). TCNQ vapor is generated through heating TCNQ powder. The TCNQ vapor was transfer by argon gas to react with metal Cu(Ag) on

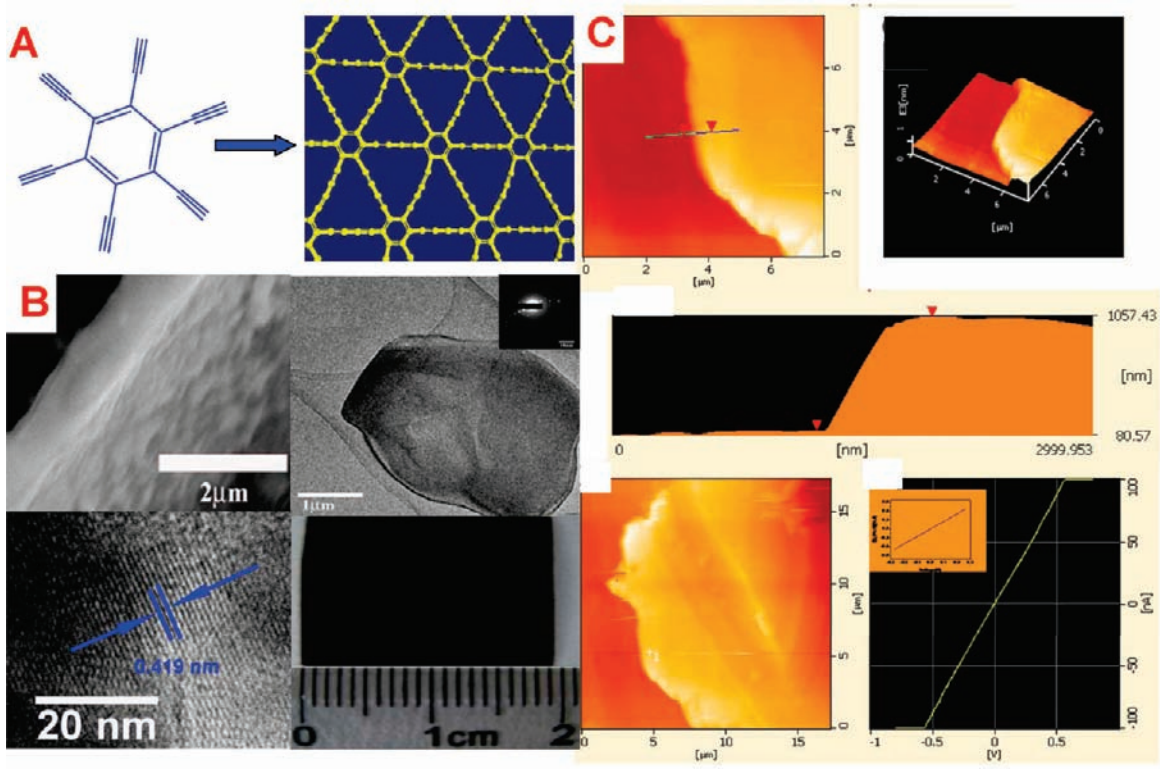

FIGURE 8. (A) Schematic outline of synthesizing graphdiyne nanoscale films, (B) SEM, TEM, HRTEM, and photographic images of a large area graphdiyne film, and (C) AFM images and the corresponding *I*−*V* curve. The inset is the *I*−*V* curve of graphdiyne films measured on the device.

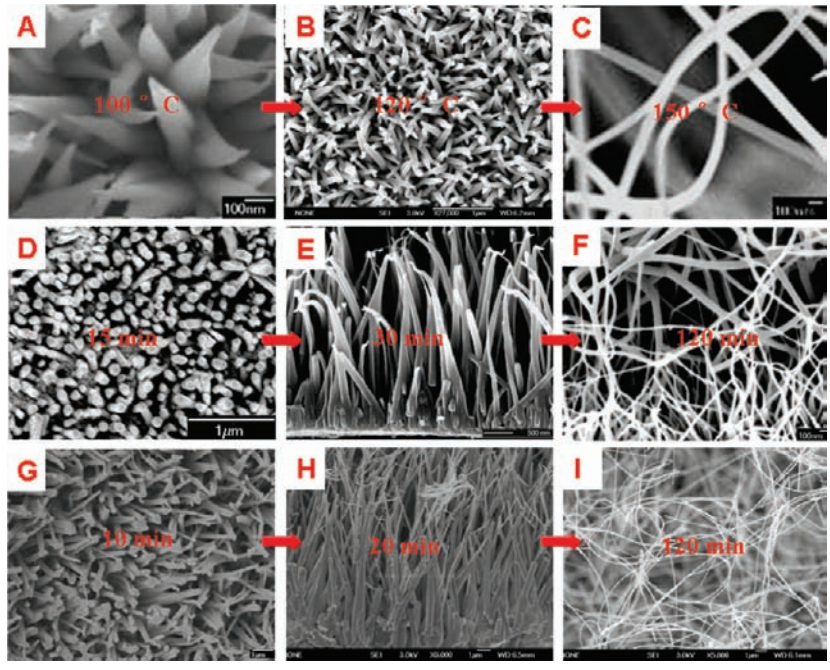

FIGURE 9. SEM images of CuTCNQ nanostructure arrays prepared (A−C) at different temperature and (D−F) at different reaction times and (G−I) AgTCNQ nanwire arrays prepared at different reaction times.

the surface of the Cu(Ag) foil to form large-scale Cu(Ag)TCNQ films filled with their oriented nanowires. The concentration of TCNQ vapor is a key factor in controlling the morphology and size of the CuTCNQ complexes, where the concentrations of TCNQ vapor can be controlled by adjusting the heating velocity (Figure 10).[30] The size of Cu(Ag)TCNQ 1D nanostructures were controlled by adjusting the temperature and time of reaction. As shown in Figure 9A−F, the diameter of the

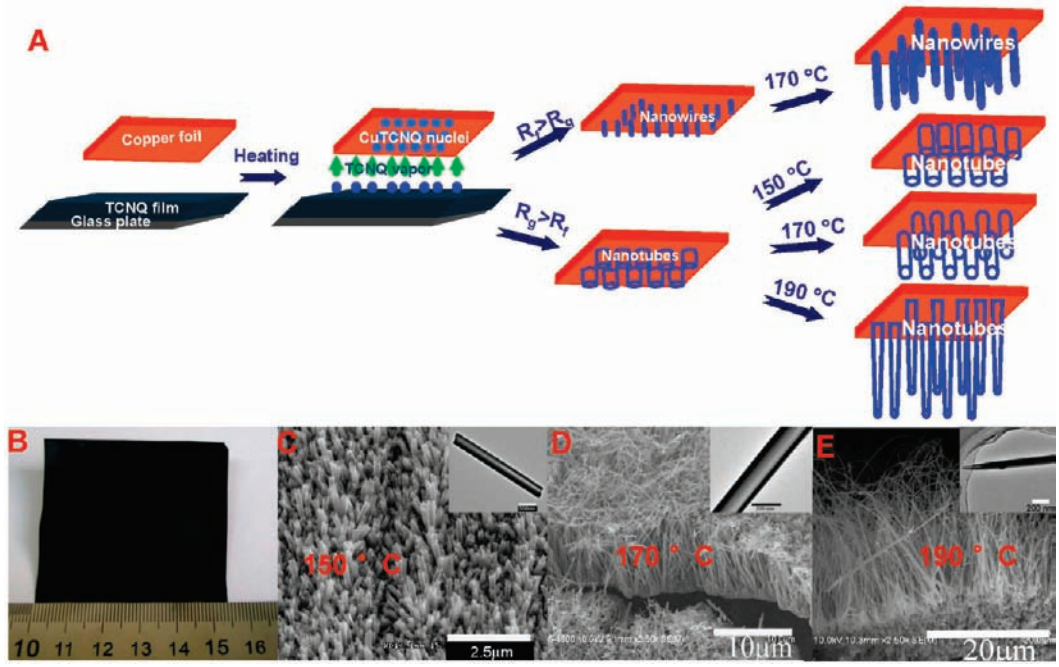

FIGURE 10. (A) Schematic illustration of the growth of CuTCNQ nanostructure arrays on Cu foil, (B) photograph of large-scale CuTCNQ nanotube arrays, and (C−E) SEM images of CuTCNQ nanowire arrays prepared at different temperatures.

CuTCNQ nanowire decreased and the length of the CuTCNQ nanowire increased with increasing the temperature and time of reaction. This also offered possibilities for fabrication of patterned CT complex arrayed films by vapor−solid-phase reactions between TCNQ and patterned Cu layers on silicon substrates.[29] CuTCNQ nanorods were obtained to grow on thick copper patterns (65 and 70 nm), and nanoparticles grow on thin copper pattern (26 and 37 nm). The growth orientation of CuTCNQ nanorods was further controlled by depressing the vertical growth with a multilayer metal structure. These nanowire arrays exhibited excellent FE properties with E_{to} of 2.58 and 3.13 V μm^{-1} for AgTCNQ and CuTCNQ, respectively. The values of E_{to} are much lower than those of most organic semiconductor nanowires and many inorganic nanomaterials. Remarkable morphology- and size-dependence of FE properties of CuTCNQ nanostructures were observed. The FE property of the nanotube is excellent in these CuTCNQ anostructures due to the small emitter radius (thickness of nanotube wall 10−30 nm). The FE properties of nanowires and nanorods are better than those of nanoparticles because of their smaller diameters. For the same nanostructures, the FE property was determined by the aspect ratio. Thus, longer length and smaller diameter are favorable to enhance the FE property. Devices based on these highly ordered CuTCNQ nanotube arrays were fabricated on Cu foils (Figure 11) and displayed excellent electrical-switching effects.[30] The CuTCNQ 1D nanostructure arrays exhibited morphology- and size-dependent electric-switching properties. The ON/OFF ratio of CuTCNQ nanowires is 4, which is less than that of CuTCNQ nanotubes (70 and 1100) due to the confined heat effect. Longer CuTCNQ nanotube arrays showed a high ON/OFF ratio of about 1100 because the longer nanotube is beneficial for efficient heat dissipation (Figure 11A).

The outstanding current density and low turn-on field of our examined organic CT complexes encouraged us to synthesize new structures of metal−organic CT complexes for applications in further field emitters. Tetracyanoanthraquinodimethane (TCNAQ) shows more efficient electron-acceptor properties than TCNQ and has been extensively studied in conjugated polymers. Recently, a novel CT complex Cu-TCNAQ has been successfully synthesized in large-area nanostructured films.[32] Instead of solid- or vapor−solid-phase reactions, controllable synthesis of Cu-TCNAQ nanowires or nanowalls was carried out in acetonitrile and acetone solutions. The nanowires, 100 nm in diameter and several micrometers in length, were observed to entangle with each other and to be built up from bunches of 1D nanowires with diameters of several tens of nanometers. TEM analysis indicated that the nanowires were polycrystalline. The nanowalls were formed by controlling growth in acetone. Investigation of SAED and XRD definitely showed the crystallinity of the nanowalls. The unique morphology and geometric shape of Cu-TCNAQ made them promising candidates for FE applications (Figure 11C). The E_{to} for the nanowire film and nano-

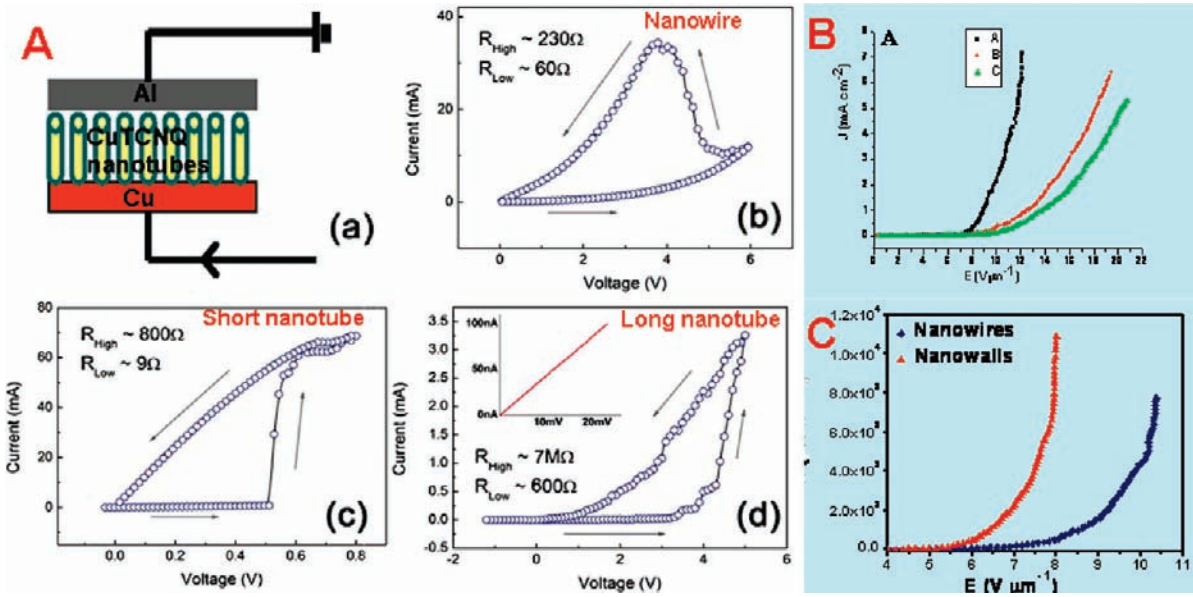

FIGURE 11. (A) Illustration of the circuit of device under testing and typical *I*−*V* curves for CuTCNQ nanotube and nanowire arrays and (B) their FE properties, and (C) *J*−*E* curve of Cu-TCNAQ nanowires and Cu-TCNAQ nanowalls.

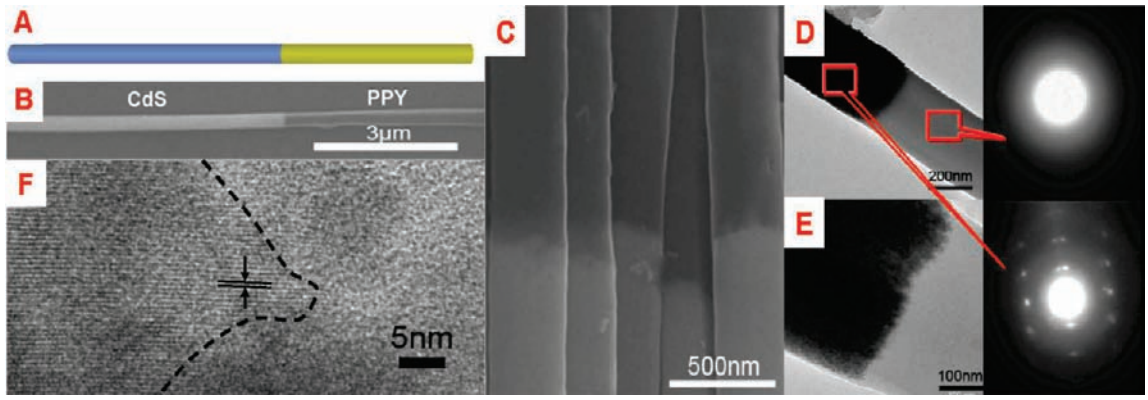

FIGURE 12. CdS−PPY nanowires: (A) model; (B, C) SEM images; (D, E) TEM images and SAED pattern; (F) HRTEM image.

wall film are 5.6 and 4.5 V μm^{-1}, respectively, and the corresponding E_{thr} was achieved at about 8.6 and 6.4 V μm^{-1}. A higher maximal current density of 10.9 mA cm^{-2} for the nanowall film was obtained, while the maximal current density of the nanowire film was 7.7 mA cm^{-2}, demonstrating the much better FE properties of the nanowalls than of the nanowires.

4. Self-Assembled Aggregate Nanostructures of Low-Dimensionality Organic/Inorganic Hybrids

As interesting nanostructures, hybrid nanocomposites are able to control many physical properties and tune size and shape of nanostructures. Many new concepts for controlling synthesis of hybrid nanocomposites have been studied, such as metal−metal junctions, metal−polymer junctions, inorganic semiconductor junctions, inorganic semiconductor−metal junctions, and semiconductor−carbon nanotube junctions.[33−35] However, how to combine organic semiconductors and inorganic semiconductors to produce uniformity of the size and shape at nanoscale with unique properties is still a challenge. Template synthesis of organic or organic/inorganic hybrid nanostructures has attracted much attention because it is a versatile and template controlled approach. In this section, we give an overview of the present studies of organic/inorganic semiconductor hybrid 1D nanostructures. Organic/inorganic semiconductor p−n junction nanowires were fabricated by using a template assisted *in situ* electropolymerization method (Figure 12).[36] PPY (polypyrrole) was used as P-type organic semiconductor and CdS as an N-type inorganic semiconductor. We first deposited CdS nanowires with a length of 10 μm into the anodic aluminum oxide (AAO) template by an electrochemistry method. Then the AAO template containing CdS nanowires was used as a working electrode to

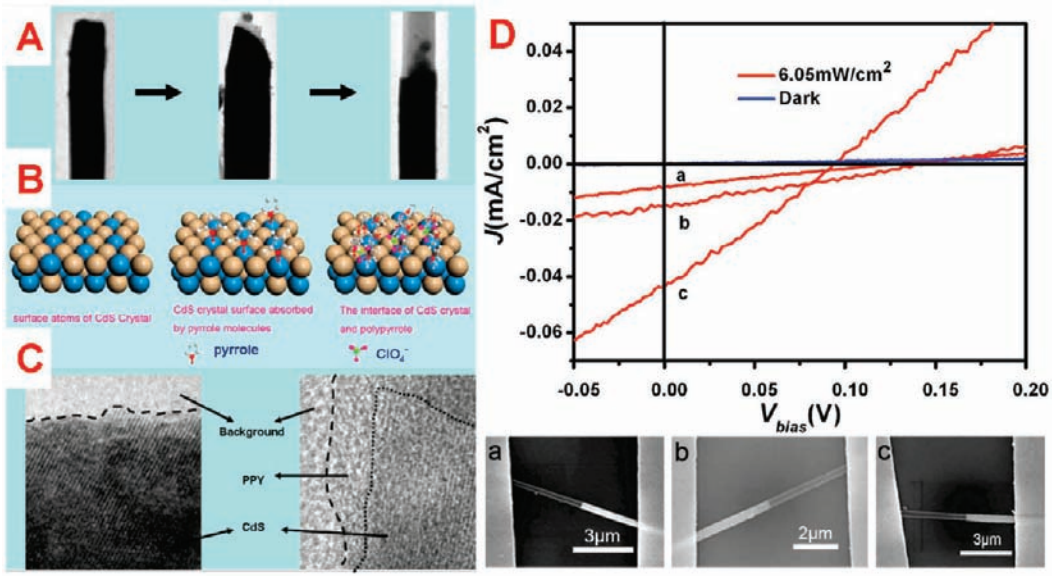

FIGURE 13. (A) TEM images of CdS−PPY p−n juction nanowire in different growth stages; (B) models of CdS surface in different growth stages; (C) HRTEM image of CdS crystal and CdS−PPY interface, and (D) *J*−*V* data of three devices of single CdS−PPY nanowire solar cell.

continually deposit PPy for the formation of the CdS−PPY heterojunction nanowires. The formed hybrid nanowires are well-defined, with smooth surfaces and diameters of 200−400 nm (Figure 12B,C). A clear interface between organic and inorganic semiconductor was observed on a single nanowire of CdS−PPY, and the element mapping definitely demonstrated the end-to-end structure of the CdS−PPY hybrid nanowires. TEM and HRTEM images revealed the exact interface structure of the CdS−PPY, indicating the single-crystalline CdS attached firmly to amorphous PPY (Figure 12D−F). The observed lattice spacing around 0.34 nm agreed well with interplanar distance of the (002) direction parallel in the hexagonal wurtzite phase of CdS. The electrical properties of p−n junctions within the organic/inorganic hybrid nanowires were probed by the current (*I*) versus bias voltage (*V*) measurements with a top-contact device configuration. The *I*−*V* curve of an individual CdS nanowire showed that the CdS nanowires were highly insulating in the dark with the resistivity of $1.055 \times 10^7\ \Omega \cdot$cm, and photoresponse was detected along with an increase of white-light illumination power. The typical *I*−*V* curve of the PPY nanowire exhibited the semiconducting property with a resistivity of 65.2 Ω·cm. The unique phenomenon of light-controlled diode on the single CdS−PPY heterojunction nanowire was observed to exhibit a rectifying property under illumination of different light intensity. The rectification ratio of the diode at 10.0 V is the same as the ratio at 5.0 V (about 13) under 5.76 mW/cm^2 illuminations. The CdS−PPY p−n heterojunction nanowires were also fabricated into photovoltaic devices, and the photophysical properties of such nanowire devices were investigated for the first time.[37] The CdS−PPY nanowires exhibited a power conversion efficiency of 0.018% under an illumination intensity of 6.05 mW/cm^2 (Figure 13). It was believed that the novel fabrication method of the organic/inorganic semiconductor p−n junction nanowire and the remarkable performance on light-controlled diode within a single hybrid p−n junction nanowire would have great influence in both the basic research field of nanoscience and the device application field of nanotechnology.

Homogeneous hybrid organic/inorganic nanorods composed of oligo(*p*-phenylene vinylene) (OPV_3) and CdS were fabricated by a similar template method. Strong interaction between the organic and the inorganic components was indicated by the different exhibited optical properties of the CdS−OPV_3 hybrid nanorods and those of the individual component CdS nanorods and OPV_3 nanorods.[38] Also, the controlled growth of hybrid organic/inorganic core−shell and segmented nanorods was accomplished by growth processes of bottom-up and top-down based on organic semiconductor polythiophene and inorganic semiconductor CdS.[39]

Recently, we have developed a new strategy for producing supramolecular interactions at the inorganic−organic semiconductor interface of hybrid nanomaterials based on ZnO nanorods and a perylene diimide derivative (PDI) (Figure 14).[40] Inorganic−organic hybrid nanorods (ZPDI) with molecular pockets have been prepared by the assembly of ZnO nanorods and PDI. The supramolecular interactions at the inorganic−organic interface led to a novel principle for selective recognition of perylene molecules on a solid interface. The thiol−zinc bond attached the PDI molecule to ZnO nano-

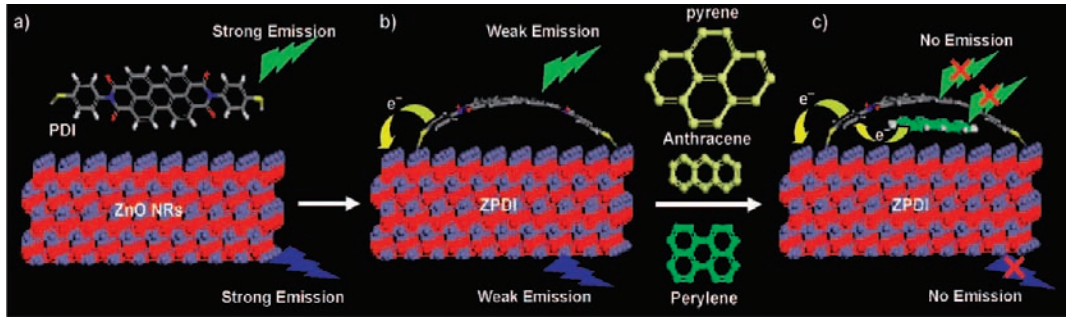

FIGURE 14. Illustration of the ZPDI sensor for perylene: (a) model of PDI and ZnO nanorods (O red, Zn gray, S yellow, N blue, H white); (b) ZPDI; (c) ZPDI with intercalated perylene.

rods to form the molecular pocket at the inorganic–organic interface. The capture of the perylene molecule by ZPDI and the supramolecular interactions at the inorganic–organic interface resulted in almost complete quenching of the emission signals of both ZPDI and perylene. Therefore, ZPDI exhibited a selective turn-off fluorescence response to perylene molecules in solution. Competition experiments with ZPDI and other polycyclic aromatic hydrocarbons to determine the selectivity of ZPDI for perylene showed an excellent selectivity for perylene over other PAHs examined. The detection limit was as low as 10^{-12} M.

5. Conclusion and Perspectives

This Account covers the trends in the synthesis, self-assembly, and aggregation structures and properties of organic molecular materials. It highlights the concept that rational design of organic molecules can be utilized to develop novel aggregate structure materials of organic conjugated molecules, which have been driven by their unique properties, as well as by the processing advantages of organic electronic materials relative to inorganic electronic materials on molecular electronic components with controlled properties. New aggregate nanostructures of organic conjugated molecules are essential for studies aimed at developing structure–property relationships needed to predict physical properties. There are encouraging results that suggest that aggregate nanostructures of organic molecular material frameworks can guide design, new nanostructures and materials of organic systems, and application of these nanomaterials across the range of compositions, sizes, shapes, and functionality on electrical, optical, and optoelectronic fields. Analysis in real earnest of the studies we describe in this Account suggests that there is still much to learn in developing construction methods of aggregate nanostructures and materials of conjugated organic molecules and, furthermore, points to a number of important research challenges that would accelerate a transition toward nanoscience and nanotechnology. There are, however, several challenges that remain for efficiently directing the development of organic molecular aggregate nanomaterials. One of the most important challenges is to fabricate large-area and highly ordered 1D organic nanostructures aligned in a single direction, which can be directly applied in devices. Further advances in self-assembly techniques according to the characteristics of organic molecules are an urgent need. The design and synthesis of new high-performance, air-stable organic molecules from both p- and n-type semiconductors and construction of nanostructures with desired morphology and size using these molecules as building blocks present another challenge. The precise control of size, shape, and morphologies and understanding self-assembly processes of aggregate structures should be further developed. Meanwhile, it should not be forgotten that there is still considerable scope for improvement in classic organic molecules through investigation and optimization of their structures at nanoscale. Particularly, new or improved chemical and physical properties induced by aggregation and self-assembly will be exploited for applications of optics, electronics, and optoelectronics. Other challenges will be to achieve complex structures from assembled organic nanostructures and improved theoretical methods for prediction of their preferred aggregate geometries on nanoscale. Further development and application of this framework to the design and production of large-area ordered organic aggregate nanostructures will provide research opportunities and challenges for this field for the foreseeable future.

This work was supported by the National Nature Science Foundation of China (Grants 20831160507, 20721061, and 20873155), the National Basic Research 973 Program of China.

BIOGRAPHICAL INFORMATION

Huibiao Liu received his Ph.D. degree in 2001 at the Nanjing University. He is currently an associate professor in Prof. Yuliang

Li's group, Institute of Chemistry, Chinese Academy of Sciences (ICCAS), working on inorganic/organic hybrid nanomaterials.

Jialiang Xu received his Ph.D. degree in 2010 at ICCAS. His research focuses on organic low-dimensionality nanomaterials.

Yongjun Li received his Ph.D. degree in 2006 at ICCAS. He is currently an associate professor in Prof. Yuliang Li's group, ICCAS, working on the design and synthesis of functional organic molecules.

Yuliang Li is a Professor at the Institute of Chemistry, Chinese Academy of Sciences. His research interests lie in the fields of functional conjugated organic molecular systems, covalent and noncovalent supramolecular self-assembly systems, and fullerene chemistry, with particular focus on the design and synthesis of photoelectroactive organofullerenes and nanoscale and nanostructural materials.

FOOTNOTES

*To whom correspondence should be addressed. E-mail: ylli@iccas.ac.cn.

REFERENCES

1 Coropceanu, V.; Cornil, J.; da Silva Filho, D. A.; Olivier, Y.; Silbey, R.; Bredas, J. L. Charge Transport in Organic Semiconductors. *Chem. Rev.* **2007**, *107*, 926–952.

2 Tashiro, K.; Aida, T. Metalloporphyrin Hosts for Supramolecular Chemistry of Fullerenes. *Chem. Soc. Rev.* **2007**, *36*, 189–197.

3 Zang, L.; Che, Y.; Moore, J. F. One-Dimensional Self-Assembly of Planar π-Conjugated Molecules: Adaptable Building Blocks for Organic Nanodevices. *Acc. Chem. Res.* **2008**, *41*, 1596–1608.

4 Grimsdale, A. C.; Müllen, K. The Chemistry of Organic Nanomaterials. *Angew. Chem., Int. Ed.* **2005**, *44*, 5592–5629.

5 Lee, C. C.; Grenier, C.; Meijer, E. W.; Schenning, A. P. H. J. Preparation and Characterization of Helical Self-Assembled Nanofibers. *Chem. Soc. Rev.* **2009**, *38*, 671–683.

6 Palmer, L. C.; Stupp, S. I. Molecular Self-Assembly into One-Dimensional Nanostructures. *Acc. Chem. Res.* **2008**, *41*, 1674–1684.

7 Bong, D. T.; Clark, T. D.; Granja, J. R.; Ghadiri, M. R. Self-Assembling Organic Nanotubes. *Angew. Chem., Int. Ed.* **2001**, *40*, 988–1011.

8 Zhao, Y.; Fu, H.; Peng, A.; Ma, Y.; Liao, Q.; Yao, J. Construction and Optoelectronic Properties of Organic One-Dimensional Nanostructures. *Acc. Chem. Res.* **2010**, *43*, 409–418.

9 Lu, W.; Chen, Y.; Roy, V. A. L.; Chui, S. S.-Y.; Che, C.-M. Supramolecular Polymers and Chromonic Mesophases Self-Organized from Phosphorescent Cationic Organoplatinum(II) Complexes in Water. *Angew. Chem., Int. Ed.* **2009**, *48*, 7621–7625.

10 Cui, S.; Liu, H.; Gan, L.; Li, Y.; Zhu, D. Fabrication of Low-Dimension Nanostructures Based on Organic Conjugated Molecules. *Adv. Mater.* **2008**, *20*, 2918–2925.

11 Zhou, W.; Li, Y.; Zhu, D. Progress in Polydiacetylene Nanowires by Self-Assembly and Self-Polymerization. *Chem.—Asian J.* **2007**, *2*, 222–229.

12 Lv, J.; Liu, H.; Li, Y. Self-Assembly and Properties of Low-Dimensional Nanomaterials Based on Pi-Conjugated Organic Molecules. *Pure Appl. Chem.* **2008**, *80*, 639–658.

13 Lindsey, J. S. Synthetic Routes to meso-Patterned Porphyrins. *Acc. Chem. Res.* **2010**, *43*, 300–311.

14 Li, Y.; Li, X.; Li, Y.; Liu, H.; Wang, S.; Gan, H.; Li, J.; Wang, N.; He, X.; Zhu, D. Amphiphilic Bis-porphyrin-Bipyridinium-Palladium Complex: From Multibilayer Vesicles to Hollow Capsules. *Angew. Chem., Int. Ed.* **2006**, *45*, 3639–3643.

15 Huang, C.; Wen, L.; Liu, H.; Li, Y.; Liu, X.; Yuan, M.; Zhai, J.; Jiang, L.; Zhu, D. Controllable Growth Zero- to Multi- Dimensional Nanostructures of a Novel Porphyrin Molecule. *Adv. Mater.* **2009**, *21*, 1721–1725.

16 Huang, C.; Li, Y.; Yang, J.; Cheng, N.; Liu, H.; Li, Y. Construction of Multidimensional Nanostructures by Self-Assembly of a Porphyrin Analogue. *Chem. Commun.* **2010**, *46*, 3161–3163.

17 Huang, C.; Li, Y.; Song, Y.; Li, Y.; Liu, H.; Zhu, D. Ordered Nanosphere Alignment of Porphyrin for Improvement in Nonlinear Optical Properties. *Adv. Mater.* **2010**, *22*, 3532–3536.

18 Liu, H.; Li, Y.; Jiang, L.; Luo, H.; Xiao, S.; Fang, H.; Li, H.; ZhuD., Yu, D.; Xu, J.; Xiang, B. Imaging as-Grown [60]Fullerene Nanotubes by Template Technique. *J. Am. Chem. Soc.* **2002**, *124*, 13370–13371.

19 Gan, H.; Liu, H.; Li, Y.; Gan, L.; Jiang, L.; Jiu, T.; Wang, N.; He, X.; Zhu, D. Fabrication of Fullerene Nanotube Arrays Using a Template Technique. *Carbon* **2005**, *43*, 205–208.

20 Liu, H.; Li, Y.; Xiao, S.; Gan, H.; Jiu, T.; Li, H.; Jiang, L.; Zhu, D.; Yu, D.; Xiang, B.; Chen, Y. Synthesis of Organic One-Dimensional Nanomaterials by Solid-Phase Reaction. *J. Am. Chem. Soc.* **2003**, *125*, 10794–10795.

21 Liu, H.; Li, Y.; Xiao, S.; Li, H.; Jiang, L.; Zhu, D.; Xiang, B.; Chen, Y.; Yu, D. Control Growth of One Dimensional Nanostructures of Organic Materials. *J. Phys. Chem. B* **2004**, *108*, 7744–7747.

22 Xu, J.; Liu, X.; Lv, J.; Zhu, M.; Huang, C.; Zhou, W.; Yin, X.; Liu, H.; Li, Y.; Ye, J. Morphology Transition and Aggregation-Induced Emission of an Intramolecular Charge-Transfer Compound. *Langmuir* **2008**, *24*, 4231–4237.

23 Xu, J.; Wen, L.; Zhou, W.; Lv, J.; Guo, Y.; Zhu, M.; Liu, H.; Li, Y.; Jiang, L. Asymmetric and Symmetric Dipole-Dipole Interactions Drive Distinct Aggregation and Emission Behavior of Intramolecular Charge-Transfer Molecules. *J. Phys. Chem. C* **2009**, *113*, 5924–5932.

24 Xu, J.; Zheng, H.; Liu, H.; Zhou, C.; Zhao, Y.; Li, Y.; Li, Y. Crystal Hierarchical Supramolecular Architectures from 1-D Precursor Single-Crystal Seeds. *J. Phys. Chem. C* **2010**, *114*, 2925–2931.

25 Zhou, W.; Xu, J.; Zheng, H.; Yin, X.; Zuo, Z.; Liu, H.; Li, Y. Distinct Nanostructures from a Molecular Shuttle: Effects of Shuttling Movement on Nanostructural Morphologies. *Adv. Funct. Mater.* **2009**, *19*, 141–149.

26 Gan, H.; Liu, H.; Li, Y.; Zhao, Q.; Li, Y.; Wang, S.; Jiu, T.; Wang, N.; He, X.; Yu, D.; Zhu, D. Fabrication of Polydiacetylene Nanowires by Associated Self-Polymerization and Self-Assembly Processes for Efficient Field Emission Properties. *J. Am. Chem. Soc.* **2005**, *127*, 12452–12453.

27 Li, G.; Li, Y.; Liu, H.; Guo, Y.; Li, Y.; Zhu, D. Architecture of Graphdiyne Nanoscale Films. *Chem. Commun.* **2010**, *46*, 3256–3258.

28 Liu, H.; Zhao, Q.; Li, Y.; Liu, Y.; Lu, F.; Zhuang, J.; Wang, S.; Jiang, L.; Zhu, D.; Yu, D.; Chi, L. Field Emission Properties of Large Area Nanowires of Organic Charge Transfer Complexes. *J. Am. Chem. Soc.* **2005**, *127*, 1120–1121.

29 Liu, H.; Wu, X.; Chi, L.; Zhong, D.; Zhao, Q.; Li, Y.; Yu, D.; Fuchs, H.; Zhu, D. Tuning CuTCNQ Nanstrucutres on Patterned Copper Films. *J. Phys. Chem. C* **2008**, *112*, 17625–17630.

30 Liu, H.; Liu, Z.; Qian, X.; Guo, Y.; Cui, S.; Sun, L.; Song, Y.; Li, Y.; Zhu, D. Field Emission and Electrical Switching Properties of Large-Area CuTCNQ Nanotube Arrays. *Cryst. Growth Des.* **2010**, *10*, 237–243.

31 Ouyang, C.; Guo, Y.; Liu, H.; Zhao, Y.; Li, G.; Li, Y.; Song, Y.; Li, Y. Tuning Morphologies and Field-Emission Properties of $CuTCNQF_4$ and $AgTCNQF_4$ Nanostructures. *J. Phys. Chem. C* **2009**, *113*, 7044–7051.

32 Cui, S.; Li, Y.; Guo, Y.; Liu, H.; Song, Y.; Xu, J.; Lv, J.; Zhu, M.; Zhu, D. Fabrication and Field Emission Properties of Large-Area Nanostructures of Organic Charge-Transfer Complex of Cu-TCNAQ. *Adv. Mater.* **2008**, *20*, 309–313.

33 Park, S.; Chung, S. W.; Mirkin, C. A. Hybrid Organic—Inorganic, Rod-Shaped Nanoresistors and Diodes. *J. Am. Chem. Soc.* **2004**, *126*, 11772–11773.

34 Kovtyukhova, N. I.; Mallouk, T. E. Nanowire p-n Heterojunction Diodes Made by Templated Assembly of Multilayer Carbon-Nanotube/Polymer/Semiconductor-Particle Shells around Metal Nanowires. *Adv. Mater.* **2005**, *17*, 187–192.

35 Liu, X.; Li, Y. One-Dimensional Hybrid Nanostructures with Light-Controlled Properties. *Dalton Trans.* **2009**, *xxx*, 6447–6457.

36 Guo, Y.; Tang, Q.; Liu, H.; Zhang, Y.; Li, Y.; Hu, W.; Wang, S.; Zhu, D. Light-Controlled Organic/Inorganic P—N Junction Nanowires. *J. Am. Chem. Soc.* **2008**, *130*, 9298–9299.

37 Guo, Y.; Zhang, Y.; Liu, H.; Lai, S.-W.; Li, Y.; Li, Y.; Hu, W.; Wang, S.; Che, C.-M.; Zhu, D. Assembled Organic/Inorganic p-n Junction Interface and Photovoltaic Cell on a Single Nanowire. *J. Phys. Chem. Lett.* **2010**, *1*, 327–330.

38 Guo, Y.; Li, Y.; Xu, J.; Liu, X.; Xu, J.; Lv, J.; Huang, C.; Zhu, M.; Cui, S.; Jiang, L.; Liu, H.; Wang, S. Fabrication of Homogeneous Hybrid Nanorod of Organic/Inorganic Semiconductor Materials. *J. Phys. Chem. C* **2008**, *112*, 8223–8228.

39 Guo, Y.; Liu, H.; Li, Y.; Li, G.; Zhao, Y.; Song, Y.; Li, Y. Controlled Core—Shell Structure for Efficient Enhancing Field-Emission Properties of Organic-Inorganic Hybrid Nanorods. *J. Phys. Chem. C* **2009**, *113*, 12669–12673.

40 Liu, H.; Zuo, Z.; Guo, Y.; Li, Y. J.; Li, Y. L. Supramolecular Interactions at the Inorganic-Organic Interface in Hybrid Nanomaterials. *Angew. Chem., Int. Ed.* **2010**, *49*, 2705–2707.